

Carbon-13 Chemical Shift Tensors in Polycyclic Aromatic Compounds. 6.¹ Single-Crystal Study of Perylene

Robbie J. Iulucci,[†] Cu G. Phung,[†] Julio C. Facelli,[‡] and David M. Grant^{*,†}

Contribution from the Department of Chemistry and the Utah Supercomputing Institute, University of Utah, Salt Lake City, Utah 84112

Received December 4, 1995[⊗]

Abstract: The 40 chemical shift tensors of single-crystal perylene in the α crystalline form have been determined with a precision of 0.30 ppm using ¹³C chemical shift–chemical shift correlation spectroscopy. The in-plane anisotropy of these tensors describes the delocalization of π -electrons at the inner α positions, which is similar to that found in biaryl linkages rather than typical bridgehead carbons. Molecular distortions, originated in intermolecular interactions and associated with chemical shifts of up to 5 ppm in similar carbons of perylene, have been detected indicating that the accuracy in the shift tensors measured in this study is adequate to probe crystalline effects upon the electronic and molecular structure. The systematic tilt observed in the orientation of the smallest principal components, δ_{33} , supports the X-ray observation that the molecules bend about their long axis by 1–2°. Chemical shift calculations, using *ab initio* methods, are in good agreement with the experimental tensors and provide insight into the observed variation of chemical shifts in terms of molecular geometry.

Introduction

From the original NMR spectrum of ethanol,² where a variation in the resonance frequencies was first observed for different protons in the same molecule, it has been demonstrated that chemical shifts provide an invaluable structural tool. Recent advances in technology, including new NMR experiments and molecular modeling methods, have amplified the successes of NMR as a premier tool for elucidating molecular structure. Recent work includes such diverse examples as the determination of dihedral angles in retinoic acids³ by rotational resonance NMR, the determination of protein's secondary and tertiary structural influence on chemical shifts via *ab initio* calculations,⁴ dipolar spectroscopy used to determine the structure of reactive intermediates trapped in inert matrices,^{5,6} etc. The work presented here in the solid state further demonstrates the sensitivity of the chemical shift on local electronic structure and highlights its potential for quantitative structural analysis.

The intimate relationship between chemical shift tensors and the electronic structure of aromatic molecules has been treated earlier in this group. The sensitivity of the chemical shift tensor to structural features is particularly noticeable in aromatic compounds where the polarizability of π -electrons results in ¹³C chemical shift tensors with overall anisotropies of about 200 ppm. Single-crystal NMR measurements provide complete

¹³C chemical shift tensors, and the increased resolution in the 2D chemical shift–chemical shift (CS-CS), correlation method^{9,10} allows the study of crystals containing 50–100 magnetically different nuclei per unit cell. The redundant data provided by the crystal symmetry increases the number of independent observations of a given shift tensor enabling the calibration of the magnetic field directions in the single-crystal sample and improving the precision of the shift measurements to better than 0.5 ppm.

Calculations of the chemical shift tensors, using *ab initio* methods, are needed to reveal the structural information contained in these NMR data. Fortunately, recent computational advances^{11–13} enable such theoretical methods to correlate experimental ¹³C chemical shift tensors of aromatic molecules^{1,7,8} with root mean square (rms) chemical shift distances¹⁴ of 4–6 ppm. This level of agreement between calculated and experimental tensors makes the uncertainties in the structural parameters, necessary for the calculations, a limiting factor in the analysis of chemical shifts. Thus, chemical shift tensor data promise to become an important tool for addressing certain fine details of solid-state structure.

This perylene study is a natural extension to the previous work on ¹³C chemical shift tensors in representative polycyclic aromatic hydrocarbons (PAH), e.g., pyrene,¹⁵ naphthalene,¹⁶ phenanthrene,¹⁷ substituted naphthalene compounds,¹⁸ and acenaphthene.¹ Moreover, perylene is one of the simplest PAH

[†] Department of Chemistry.

[‡] Utah Supercomputing Institute.

[⊗] Abstract published in *Advance ACS Abstracts*, May 1, 1996.

(1) Previous paper in this series, Iulucci, R. J.; Alderman, D. W.; Facelli, J. C.; Grant, D. M. *J. Am. Chem. Soc.* **1995**, *117*, 2336.

(2) Arnold, J. T.; Dharmatti, S. S.; Packard, M. E. *J. Chem. Phys.* **1951**, *19*, 501.

(3) McDermott, A. E.; Creuzet, F.; Gebhard, R.; van der Hoef, K.; Levitt, M. H.; Herzfeld, J.; Lugtenburg, J.; Griffin, R. G. *Biochemistry* **1994**, *33*, 6129.

(4) de Dios, A. C.; Pearson, J. G.; Oldfield, E. *Science* **1993**, *260*, 1491.

(5) Orendt, A. M.; Arnold, B. R.; Radziszewski, J. G.; Facelli, J. C.; Malsch, K. D.; Strub, H.; Grant, D. M.; Michl, J. *J. Am. Chem. Soc.* **1988**, *110*, 2648.

(6) Orendt, A. M.; Facelli, J. C.; Radziszewski, J. G.; Horton, W. J.; Grant, D. M.; Michl, J. *J. Am. Chem. Soc.* **1996**, *118*, 846.

(7) Grant, D. M.; Liu, F.; Iulucci, R. J.; Phung, C. G.; Facelli, J. C.; Alderman, D. W. *Acta Crystallogr.* **1995**, *B51*, 540.

(8) Facelli, J. C.; Grant, D. M. *Nature* **1993**, *365*, 325.

(9) Carter, C. M.; Alderman, D. W.; Grant, D. M. *J. Magn. Reson.* **1987**, *73*, 114.

(10) Sherwood, M. H.; Alderman, D. W.; Grant, D. M. *J. Magn. Reson.* **1989**, *84*, 466.

(11) Wolinski, K.; Hinton, J. F.; Pulay, P. *J. Am. Chem. Soc.* **1990**, *112*, 8251.

(12) Chesnut, D. B. In *Annual Reports on NMR Spectroscopy*; Webb, G. A., Ed.; Academic Press: New York, 1994; Vol. 29, p 71.

(13) Facelli, J. C. In *Encyclopedia of NMR*; Grant, D. M.; Harris, R. K., Eds.; John Wiley: London, 1996; p 4327.

(14) Alderman, D. W.; Sherwood, M. H.; Grant, D. M. *J. Magn. Reson.* **1993**, *A101*, 188.

(15) Carter, C. M.; Facelli, J. C.; Alderman, D. W.; Grant, D. M. *J. Am. Chem. Soc.* **1987**, *109*, 2639.

(16) Sherwood, M. H.; Facelli, J. C.; Alderman, D. W.; Grant, D. M. *J. Am. Chem. Soc.* **1991**, *113*, 750.

(17) Soderquist, A.; Hughes, C. D.; Horton, W. J.; Facelli, J. C.; Grant, D. M. *J. Am. Chem. Soc.* **1992**, *114*, 2826.

where the Kekule structures predict the confinement of the π -electrons to the naphthalene residues, therefore this study of its ^{13}C chemical shift tensors provides further insight into the localization—delocalization aspect of π -electron structure. The crystal structure of perylene in the α form^{19,20} is also favorable for these studies because the existing symmetry relationship among the four chemically equivalent molecules in the unit cell increases the precision of the tensor determinations. On the other hand, the unit cell symmetry of the α form leaves each individual perylene molecule with C_i symmetry, making chemically similar carbons in a given molecule crystallographically different, allowing the influence of crystalline forces on the chemical shift tensors to be studied in otherwise chemically similar carbons.

Experimental Section

Crystal. Perylene, commercially obtained from Aldrich, was purified by sublimation followed by zone refining. The Bridgman method²¹ was used to grow a cylindrical single crystal 5 mm in diameter and 4 cm in length. The crystal was then grounded to fill 5 mm of a shortened 5-mm NMR tube. Epoxy glue was used to mount the crystal in a fixed position in the NMR tube and the probe armature. The α form of perylene is stable at all temperatures up to its melting point while the β form is only stable below 140 °C. Thus, the crystal used in this study, which was grown from the melt, should belong to the α form. This was confirmed by its bright yellow/orange color which is characteristic of the α form in contrast with the greenish-yellow color characteristic of the β form.²²

Spectroscopy. Six 2D spectra were acquired at room temperature on a Bruker CXP-200 spectrometer. The operating frequencies for ^{13}C and ^1H are 50.304 and 200.06 MHz, respectively. Previous publications describe the instrumentation including probe, sample flipping mechanism, pulse sequence, calibration of field directions, and external referencing to TMS.^{6,10} A 5-ms contact time was sufficient to achieve cross polarization. The evolution dimension was incremented in 125 real and imaginary steps with 8 transients per increment. The spectral windows in the evolution and acquisition dimensions were 15385 and 38462 Hz, respectively. The carrier frequency was set at the center of the evolutionary spectral window to observe -25 to 280 ppm shifts with respect to TMS. The acquisition dimension was digitized with 512 points. The 2D mixing time was 35 ms, a time which is sufficient to rotate the sample and to apply the necessary rf pulses. The proton decoupling field strength was 89 kHz, and a flip back pulse restored the proton magnetization after the acquisition period. A recycle delay of 240 s provided the optimal signal to noise for a given experiment. Each 2D spectrum was obtained in 6 days.

The ^{13}C free induction decay, transferred to a VAX 3100 for analysis, was zero filled to produce a 1024 by 1024 point spectrum. The quadrature hypercomplex data set, using a 75-Hz Gaussian line broadening, was processed to produce pure absorption mode spectra with quadrature in both the evolution and acquisition dimensions. The position of each spectral peak in the 2D contour plots was determined from the highest pixel in the vicinity of the peaks. Before line broadening, the peak width at half height was typically 0.7 ppm.

Molecular Symmetry Considerations

Reference Frames. Three Cartesian reference frames are used throughout this study: the sample frame, the unit cell frame, and the molecular frame. The XYZ sample frame, in which the data were acquired, is arbitrarily defined by the

(18) Orendt, A. M.; Sethi, N. K.; Facelli, J. C.; Horton, W. J.; Pugmire, R. J.; Grant, D. M. *J. Am. Chem. Soc.* **1992**, *114*, 2832.

(19) Camerman, A.; Trotter, J. J. *Proc. R. Soc. London, A* **1964**, *279*, 129.

(20) Donaldson, D. M.; Robertson, J. M.; White J. G. J. *Proc. R. Soc. London, A* **1953**, *220*, 311.

(21) Sherwood, J. N. In *Purification of Inorganic and Organic Materials; Techniques of Fractional Solidification*; Marcel Dekker: New York, 1969; Chapter 15.

(22) Tanaka, J. *Bull. Chem. Soc. Jpn.* **1963**, *36*, 1237.

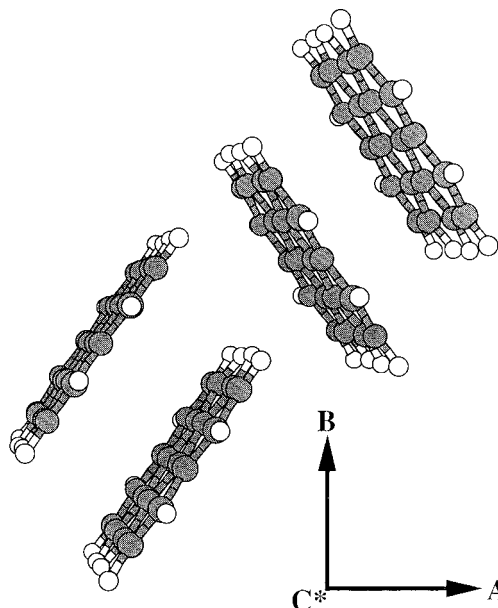


Figure 1. Unit cell of perylene in the α form showing the orthogonal axes, A , B , and C^* . The four molecules in the unit cell are all symmetry related (see text), but each individual molecule fails to exhibit any symmetry.

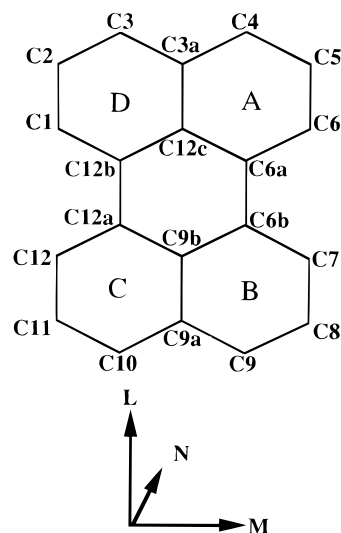


Figure 2. Numbering of the carbon positions and the perylene molecular frame used in this paper. The molecular frame was defined according to the X-ray study.¹⁹

mounting of the crystal in the NMR probe. The axes of the crystallographic unit cell are designated by A , B , and C^* and shown in Figure 1. The molecular frame with axes labeled L , M , and N (see Figure 2) is defined in the diffraction study¹⁹ with L placed on the long axis of the molecule; N is perpendicular to the plane determined by the best planar fit of the carbon coordinates, and M is orthogonal to both L and N . Diffraction data provide the necessary transformation between the unit cell and molecular frames (see Figures 1 and 2 for the spatial relationships between these two frames).

Crystal Symmetry. The α form of the perylene crystal belongs to the $P2_1/a$ space group and has four molecules per unit cell.^{19,20} The four molecules appear in the unit cell, shown in Figure 1, as molecular pairs with an inversion center relating the two molecules. This inversion symmetry reduces the effective number of molecules from four to two and decreases the number of magnetically different ^{13}C nuclei in the unit cell from 80 to 40. The four molecules in the two pairs relate to

each other by a 2-fold screw axis involving the B axis and the AC glide plane. Thus, the 40 magnetically different nuclei also divide into two sets of 20 congruent nuclei that may each be identified with the 20 carbons of one of the two magnetically different perylene molecules. The crystal symmetry establishes the relationship between sets of congruent nuclei and is readily manifested in the corresponding chemical shift tensors. In the unit cell frame, these congruent pairs of tensors are identical except as differentiated by the algebraic sign of two off-diagonal tensor elements, δ_{AB} and δ_{BC} . Thus, while only one congruent set of the tensors need be reported, the independent measurement of both sets decreases the overall errors. The composite tensors reported here correspond to an average of the two sets. This redundant information also enables a precise calibration of the magnetic field directions and provides important information on the spatial relationship between the sample and unit cell reference frames.

Molecular Symmetry. It is important to point out that the α crystalline structure imposes no symmetry constraints on the structure of a given perylene molecule. Due to intermolecular interactions, the carbon positions in a given molecule no longer relate to each other by the D_{2h} molecular symmetry of an isolated perylene molecule. While the structures are no longer equivalent, they continue to be chemically very similar. According to diffraction studies,^{19,20} the structural deviations from D_{2h} symmetry in the crystal are only modest, and it is not surprising that the tensors for chemically similar nuclei reflect this near symmetry. Nonetheless, the crystal packing clearly breaks the D_{2h} symmetry in the measured chemical shift tensors and this reduction in symmetry is readily visible from the splitting between chemically similar carbon peaks in the 2D spectrum. Otherwise the inversion element of D_{2h} symmetry would force a degeneracy on the spectrum reducing the 20 peaks to 10.

Although the orientations of principal axes in inversion related tensors of a molecule with nearly D_{2h} symmetry are almost identical, the high precision of the NMR frequencies renders the principal values measurably different. While this similarity of inversion related carbons sometimes leaves the tensor assignments ambiguous, minor but characteristic differences in other cases can be attributed to small but systematic distortions in the crystalline molecular structure. The X-ray study¹⁹ suggests a systematic bowing of the carbon network about the long axis (L) of the molecule. With only this deformation present, the tensors would reflect a C_{2v} molecular symmetry and the principal axis system (PAS) of the independent nuclei could be expected to tilt in response to this deviation from planarity. Additional out-of-plane distortions, along with the bending about the L axis, were found to reduce further the symmetry of a given perylene molecule, and the experimental NMR data are analyzed below to assay their deviation from hypothetical D_{2h} , C_{2v} , and C_2 symmetries. Such deviations from the C_i crystallographic symmetry of a single perylene molecule give a quantitative assessment of the molecular distortions of perylene in the α form.

Reference Frame Transformations. The symmetry relationship between congruent nuclear pairs completely determines, within the ambiguity of its algebraic sign, the orientation of the B crystal axis in the sample frame. However, the orientation of the A and C axes can only be extracted from the NMR data with the aid of X-ray data.¹⁹ Diffraction data and the NMR precedent indicating that the orientation of δ_{33} principal axes lie along the normals to the aromatic plane is sufficient to establish, within the experimental limitations, the relationship between the unit cell and sample frame. Since individual δ_{33} orientations in perylene may vary from one another by as much

as 5° , the average δ_{33} direction of all 20 carbons was used to establish the preferred orientation about B of the A and C^* axes.

The transformation from the sample frame to the unit cell, alternatively, may be obtained by correlating calculated shielding tensors to the experimental shift tensors. By systematically varying the numerical transformation between the sample and unit cell frames, the rms chemical shift distance¹⁴ between calculated and experimental shifts may be minimized as a function of the orientation of the A and C^* axes, defined in terms of a rotation angle about B . Within the uncertainty of the NMR measurements, this minimization procedure reproduces the same B -axes rotation as determined from combining the average δ_{33} direction in the tensor data and the average of the aromatic plane normals found in X-ray data.

To finalize the transformation of tensors from the unit cell frame into the molecular frame, first the average δ_{33} orientation along N was determined directly from the directional cosines of δ_{33} in the unit cell frame. With the N vectors identified in the unit cell frame, the orientation of the L and M axes was determined by the rotation about N which minimizes the rms distance between chemically similar tensors assuming an effective C_{2v} molecular symmetry.

Theoretical Calculation of the Chemical Shift Tensors

Quantum mechanical calculations of the ^{13}C chemical shift tensors used the GIAO method²³ in the TEXAS 93 program¹¹ with the Dunning²⁴ D95, D95V, D95*, and D95V* basis sets. The molecular geometries, used as input for these calculations, were taken from the X-ray diffraction structure¹⁹ and from structures obtained by quantum mechanical optimizations performed with the Gaussian 92 program.²⁵ All of the calculations were done for isolated molecules without taking into account possible intermolecular interactions. The slope and intercept for the correlations between calculated and experimental chemical shifts are comparable for various basis sets using the X-ray structure, the X-ray structure with optimized proton positions, and a fully optimized carbon and hydrogen structure. Interestingly, for the optimized structure the rms distance favors slightly the D95V basis set, and because of its time efficiency, this basis was used for most of the calculations. Figure 3 gives a correlation plot of the calculated versus experimental shifts in the icosahedral representation¹⁴ to illustrate visually the success of the calculations using the fully optimized structure.

As discussed above, a convenient way to unravel the large amounts of experimental data, reported here, utilizes the results of theoretical calculations of nuclear shieldings to assign the experimental chemical shift tensor data. By comparing the various measured chemical shift tensors with the theoretically derived tensors, one selects as the best assignment the permutational combination of measured versus theory that yields the smallest rms scatter in the correlation. This approach not only characterizes the overall quality of the fit but also establishes the preferred tensor assignments for the various nuclei. Systematic errors in the correlation plots are expected to affect primarily the slope and intercepts, whereas the uncertainties in the molecular structure parameters appear to impact the plot's scatter.

(23) Ditchfield, R. *Mol. Phys.* **1974**, *27*, 789.

(24) Dunning, T. H.; Hay, P. J. In *Methods of Electronic Structure Theory*; Plenum: New York, 1977.

(25) Frisch, M. J.; Trucks, G. W.; Head-Gordon, M.; Gill, P. M. W.; Wong, J. B.; Foresman, J. W.; Johnson, B. G.; Schlegel, H. B.; Rob, M. A.; Replogle, E. S.; Gomperts, J. L.; Andrees, J. L.; Raghavachari, K.; Binkley, J. S.; Gonzales, C.; Martin, R. L.; Fox, D. J.; Defrees, D. J.; Baker, J.; Stewart, J. J. P.; Pople, J. A. Gaussian 92, Gaussian, Inc.: Pittsburgh, 1992.

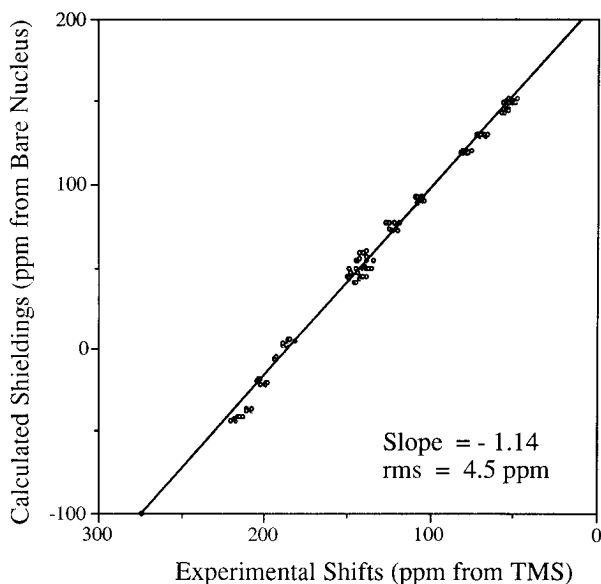


Figure 3. Correlation plot between the experimental and calculated chemical shift tensors of perylene. All the tensors are in ppm in the icosahedral representation,¹⁴ the experimental values referenced to TMS as described in the text, and the calculated values in absolute shielding values, i.e., referenced to the bare nucleus.

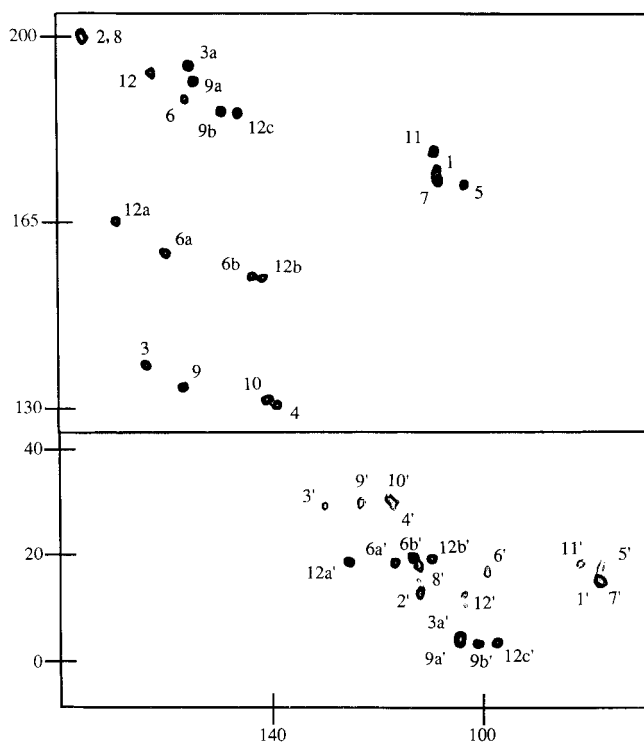


Figure 4. Expanded 2D CS-CS correlation spectrum of perylene. For clarity, the spectrum has been expanded and the center portion removed to reveal only the regions for which the spectral peaks are observed. The two clusters pertain to the different molecules in the unit cell and are well separated. The spectral peak assignments refer to the carbon positions shown in Figure 2. The different molecular assignments are differentiated here with a prime. All shifts are in ppm referenced to TMS.

Experimental Results

Spectra and Data. The analysis of chemical shift tensors determined from single-crystal NMR data using the 2D CS-CS correlation method is described adequately in ref 10. Figure 4 shows a typical 2D CS-CS spectrum of perylene. The complete data set requires six 2D spectra similar to the one in Figure 4,

which if aligned as indicated in ref 10 allows the spectral analysis and the extraction of the chemical shift tensors by tracking the individual carbon shifts between the six spectra.^{1,10} Since the δ_{33} components of the observed shift tensors show only modest variability in their values and all of them are essentially oriented perpendicular to the aromatic plane, all of the tensors pertaining to one molecule manifest similar spectral features that tend to group the peaks from a given molecule in recognizable patterns. Note, it is impossible for all six normal field directions of the CS-CS device to lie in the plane of both molecules simultaneously. Thus, in four of the six 2D spectra, the clustering of the peaks into two groups is readily visible, and the resonances from individual molecules can be separated relatively early in the assignment process thereby simplifying the overall strategies for spectral analysis.

A prominent spectral feature readily observed in Figure 4 for perylene is the departure of the chemical shift tensors from the hypothetical D_{2h} symmetry. For instance, the splittings of peaks corresponding to tensors related to each other through the near inversion center of the molecule are as large as 11 ppm along the horizontal axis of the 2D spectra shown in Figure 4. This demonstrates that the crystalline effects, direct and indirect, are significantly different for chemically similar carbons that would be related otherwise by inversion symmetry in an ideal D_{2h} molecule. Therefore, the 2D spectrum of perylene in Figure 4 demonstrates dramatically the ability of NMR data to observe crystalline effects in the molecular structure.

The chemical shift tensors of the α form of perylene are presented in Tables 1 and 2. In Table 1, the tensors are given in the Cartesian representation for the unit cell reference frame. The trace or isotropic value of the tensors, δ_{iso} , is also reported along with the isotropic shifts, δ_{liq} , from liquid studies.²⁶ In all cases the values measured here are within about 2 ppm of the literature liquid values. This deviation from liquid shifts is however measurable and reflects the importance of crystal effects on the chemical shift. The principal values and their directional cosines relative to the molecular frame are reported in Table 2. The numbering in both tables is according to the molecular scheme given in Figure 2 and the assignments have been made as described below.

Assignments. The assignment of the measured chemical shift tensors to the 20 unique carbon positions was first achieved by assigning the tensors to one of the six chemically similar positions, i.e. inner and outer α carbons, β carbons, and bridgehead carbons. As the chemical shift variations of similar nuclei differ only by crystalline effects, similar shift tensors may be grouped according to their isotropic and principal shift values.

The easiest tensors to group are those assigned to bridgehead carbons, which have a small anisotropy between δ_{11} and δ_{22} and come in pairs of carbons instead of sets of four carbons. The tensors of the two types of bridgehead carbons, outer bridgehead positions (C_{3a} and C_{9a}) and inner bridgehead positions (C_{9b} and C_{12c}), are assigned by their δ_{ave} values that compare well with the corresponding liquid-state shifts. The δ_{iso} of the four inner β positions (C_1 , C_6 , C_7 , and C_{12}) are the four lowest frequency shifts and may be grouped confidently on the basis of their unique isotropic shift values. This feature was confirmed by the liquid shifts, δ_{liq} , which are 6.3 ppm smaller than the next closest value. The inner α positions (C_{6a} , C_{6b} , C_{12a} , and C_{12b}) are distinguished by a unique δ_{22} value of about 160 ppm, which is also similar to the δ_{22} in alkyl-substituted carbons.¹⁸ The outer β positions (C_2 , C_5 , C_8 , and

(26) Karcher, W. In *Spectral Atlas of Polycyclic Aromatic Compounds: Including Data on Occurrence and Biological Activity*; Kluwer Academic Publishers: Dordrecht, Boston, 1988.

Table 1. ^{13}C Chemical Shift Tensors of Perylene in the Unit Cell Reference Frame^a

	δ_{AA}	δ_{BB}	δ_{CC}	δ_{AB}	δ_{BC}	δ_{CA}	δ_{iso}	δ_{liq}^b
inner β								
C1	77.37	127.47	155.77	90.46	15.16	28.81	120.20	120.23
C6	62.09	132.46	163.22	80.65	-38.87	-5.78	119.26	120.23
C7	66.54	141.66	158.63	85.18	17.29	29.07	122.28	120.23
C12	67.68	129.25	165.38	81.91	-37.51	-10.36	120.77	120.23
outer β								
C2	69.94	133.78	176.61	82.66	-46.88	-14.11	126.78	126.58
C5	77.28	141.46	167.03	89.85	25.19	35.82	128.59	126.58
C8	58.41	140.41	176.33	79.36	-46.33	-11.28	125.05	126.58
C11	80.96	133.12	165.84	92.98	23.41	34.04	126.64	126.58
inner α								
C6a	61.57	115.86	215.89	69.07	-22.21	12.62	131.11	131.32
C6b	61.81	118.86	209.53	70.46	5.12	25.13	129.92	131.32
C12a	71.12	113.39	211.63	73.52	2.78	27.89	130.91	131.32
C12b	64.27	112.80	215.66	68.93	-18.46	8.07	132.05	131.32
outer α								
C3	64.95	98.28	218.44	51.71	-16.76	10.92	127.23	127.87
C4	64.61	99.82	213.24	52.10	7.86	24.19	125.89	127.87
C9	60.21	102.51	220.56	51.33	-17.86	11.66	127.76	127.87
C10	67.76	99.12	217.04	54.31	4.69	28.18	127.97	127.87
inner BH								
C9b	61.86	131.69	191.79	91.77	-10.03	13.91	128.45	128.87
C12c	63.71	129.86	191.09	92.31	-11.95	16.48	128.22	128.87
outer BH								
C3a	64.20	135.56	201.50	94.79	-11.70	16.75	133.75	134.83
C9a	66.99	136.31	202.25	95.86	-10.57	14.81	135.18	134.83

^a The assignments of the chemical shift tensors presented here are tentative by the permutations that exchange the chemically similar positions related through the center of the molecule. See text for details. All values in ppm referenced to TMS. ^b Values from ref 26.

Table 2. Principal Values of the Chemical Shift Tensors of Perylene in the Molecular Frame^a

	δ_{11}	$\cos \theta_L$	$\cos \theta_M$	$\cos \theta_N$	δ_{22}	$\cos \theta_L$	$\cos \theta_M$	$\cos \theta_N$	δ_{33}	$\cos \theta_L$	$\cos \theta_M$	$\cos \theta_N$
inner β												
C1	212.0	-0.535	-0.845	0.022	141.3	0.845	-0.535	0.014	7.2	0.001	0.026	0.9997
C6	212.0	0.547	-0.837	-0.014	138.2	0.837	0.547	-0.007	7.5	0.013	-0.008	0.9999
C7	214.1	-0.545	-0.837	-0.039	143.2	0.838	-0.544	-0.029	9.5	0.003	-0.048	0.9988
C12	214.1	0.552	-0.833	0.018	138.3	0.834	0.553	-0.001	9.9	-0.009	0.015	0.9999
outer β												
C2	231.1	0.604	-0.797	0.013	137.4	0.797	0.604	-0.012	11.8	0.002	0.017	0.9999
C5	231.5	-0.603	-0.798	-0.012	141.8	0.798	-0.602	-0.013	12.5	0.003	-0.017	0.9999
C8	228.8	0.613	-0.790	-0.026	137.6	0.790	0.612	0.029	8.7	-0.007	-0.038	0.9992
C11	228.5	-0.596	-0.803	0.013	142.1	0.803	-0.596	0.012	9.3	-0.008	0.022	0.9997
inner α												
C6a	220.6	0.966	-0.257	-0.016	160.8	0.257	0.966	0.0	11.9	0.016	-0.004	0.9999
C6b	217.6	0.963	0.268	0.013	159.6	0.269	-0.963	-0.023	12.5	-0.006	-0.025	0.9997
C12a	219.0	0.969	-0.247	0.013	159.8	0.247	0.969	-0.011	14.0	-0.010	0.014	0.9999
C12b	220.7	-0.962	-0.272	0.016	161.9	0.272	-0.962	0.019	13.6	0.010	0.023	0.9997
outer α												
C3	220.8	0.988	-0.154	0.002	135.4	-0.154	-0.988	0.026	25.5	0.002	0.026	0.9997
C4	219.5	-0.985	-0.172	-0.015	132.2	0.172	-0.985	0.002	26.0	-0.015	-0.001	0.9999
C9	223.3	0.987	-0.163	-0.004	136.1	-0.163	-0.987	-0.011	23.9	0.002	-0.011	0.9999
C10	224.1	-0.986	-0.166	0.011	135.0	0.166	-0.986	0.015	24.9	0.009	0.016	0.9998
outer BH												
C3a	203.5	0.994	-0.108	-0.003	201.2	-0.108	-0.994	-0.004	-3.4	0.003	-0.004	0.9999
C9a	203.9	0.893	-0.449	0.008	203.5	0.449	0.894	0.0	-1.9	-0.007	0.003	0.9999
inner BH												
C9b	195.1	0.135	-0.991	-0.004	193.2	-0.991	-0.134	-0.010	-2.9	-0.009	-0.005	0.9999
C12c	194.9	0.100	-0.995	0.003	193.2	-0.995	-0.100	0.008	-3.4	0.008	0.004	0.9999

^a Shift values in ppm referenced to TMS, directional cosines to the *L*, *M*, and *N* axis depicted in Figure 2. For the assignments used here see footnote in Table 1.

C₁₁) and outer α positions (C₃, C₄, C₉, and C₁₀) are distinguished by the larger δ_{11} and δ_{33} shifts, respectively, having values that are very similar to those observed in naphthalene. Finally, the orientations of δ_{11} can be used to separate the outer α from outer β positions, because in protonated aromatic tensors the orientation of δ_{11} is typically within $\sim 10^\circ$ of the C-H bond directions and consequently the δ_{11} directions for outer α and β carbons differ by about 60° .

The experimental shift tensor assignment to specific carbon positions within each subgrouping proceeds with less certainty and depends upon minimizing the rms distance¹⁴ between the

experimental and calculated tensors based upon the X-ray structure.¹⁹ Only some of these assignments may be made with high confidence. The calculated tensors can easily distinguish between the chemically similar positions related by either of the two vertical molecular mirror planes (LN and MN in Figure 2) but are limited for those pairs of similar carbons related by the near inversion relationship. Except for the bridgehead positions, interchange of chemically similar carbons related by the *LN* and *MN* molecular planes drastically increases the chemical shift distance by 20–53 ppm. The near-axial symmetry of the bridgehead tensors within each type (e.g., inner

and outer) prevents one from clearly identifying, and hence assigning, these carbons related by a near-inversion operation. The rms distance, between all pairs of experimental tensors related by the near-inversion operation, is 4.29 ppm, with individual distances ranging from 1.95 to 7.39 ppm. These experimental variations clearly identify physically relevant interactions, but because ultimate assignment of similar tensors presently rests upon the quantum chemical computations, again with uncertainties of about 5 ppm, an unequivocal assignment is only tentative for carbons related by the near inversion operation.²⁷

When distortions make the tensors of similar carbons quite different the assignment of the tensors to rings A, B, C or D in Figure 2, depends primarily upon by the different orientations of their C–H bonds. In the molecular frame, the tensors of the protonated carbons, outer α , inner β , and outer β , may be assigned to either the A/C or B/D rings based on the in-plane directional cosines, $\cos \theta_1$ and $\cos \theta_m$, of δ_{11} relative to the molecular axes, which in turn relates to the orientation of the corresponding C–H bonds. Similarly, the directional cosines of δ_{11} and the orientation of the peri-bonds may be used to assign the tensors of the inner α positions to either the A/C or B/D rings. Based on the observation in the X-ray study¹⁹ that the aromatic plane bends around L , tensors in rings A and B may be separated tentatively from tensors in rings C and D by their δ_{33} orientation. As the orientation of the δ_{33} is generally perpendicular to the local aromatic plane^{15,16} and as the anisotropy between δ_{33} and either δ_{11} or δ_{22} is correspondingly large, the orientation of δ_{33} may be determined with reasonably high precision. The tilting of δ_{33} from the average δ_{33} orientation for the whole molecule is considerably greater than the measured uncertainties in these orientations and is predominantly tilted along either the plus or minus M direction, consistent with the observed X-ray molecular bending of perylene about the L axis, and consequently, the direction of δ_{33} in the C and D rings moves toward $-M$, and the tilt in the A and B rings moves toward $+M$. Chemical shielding calculations based on the distortions in the X-ray data also predict this systematic tilting of δ_{33} for a molecular bending of about 5° around the L axis. The tentative assignments in Table 2 associate the tensors with the largest tilt in δ_{33} to the carbon nuclei with the largest reported planar deformations.¹⁹

While the tensor orientations and values reported in Table 2 for perylene are based on reasonable assumptions, some care needs to be exercised in the use of these tentative assignments of very similar tensors associated with carbons related by the near inversion operation, especially the inversion-related bridgehead positions. Fortunately, the very small, though measurable, differences within inversion related tensor values make their exact assignment less physically relevant given the current limitations in chemical shift calculations. For example, the respective chemical shift distances¹⁴ between the two similar pairs of bridgehead tensors (i.e., 1.95 and 2.01 ppm) for the inner and outer bridgehead carbons fall well below the ability of the theoretical model to extract meaningful chemical information. However, such tensor differences are about three times larger than measurement uncertainties.

Error Analysis. An estimate of the overall composite error, Δ , of the data may be obtained by calculating the residuals between the individually observed shifts, ν_{obs}^i , of congruent

tensors and the average composite tensor shifts, ν_{comp}^i , obtained from the data-fitting procedures. The relation between these quantities is:

$$\Delta = \left(\sum_{i=1,N} (\nu_{\text{obs}}^i - \nu_{\text{comp}}^i)^2 / (N - D) \right)^{1/2} \quad (1)$$

where N is the number of measured shifts, 480, and D is the number of degrees of freedom, 144, due to all of the fitting parameters. This corresponds to 120 distinct tensor elements and 24 parameters, associated with the probe mechanism, that are required to describe the different orientations of the crystal in the magnetic field. This estimate of random errors ignores possible systematic shifts introduced by susceptibility corrections, systematic referencing problems, and probe misalignments. The overall composite error estimate from eq 1 is 0.30 ppm, but this value ranged from 0.07 to 0.45 ppm for the individual congruent pairs of tensors.

When the chemical shifts are presented in their PAS, it is necessary to propagate the errors treated in eq 1 into uncertainties in the principal values and directional cosines. These uncertainties, σ_{pas} , are estimated by the linear approximation

$$\sigma_{\text{pas}} = (\mathbf{P}^2 \cdot \sigma_{\text{shift}}^2)^{1/2} \quad (2)$$

where σ_{shift} is the uncertainty in determining the chemical shift and \mathbf{P} is the variance–covariance matrix. The experimental uncertainty in the chemical shift is taken as the line half width at half height, which is typically 0.6–0.8 ppm, therefore σ_{shift} is assumed to be a scalar quantity with a single value, ± 0.7 ppm. The estimate of the variance–covariance matrix contains all of the partial derivatives of the PAS elements with respect to the change in chemical shift for each field direction,

$$P_{ij} = \frac{\partial \delta_i^{\text{pas}}}{\partial f_j} \approx \frac{\Delta \delta_i^{\text{pas}}}{\Delta f_j} \quad (3)$$

where i spans both the three principal values and their corresponding directional cosines, and j spans the two different sets of X , Y , Z , XY , YZ , and ZX direction fields found in the complete data set. Each tensor is determined by a symmetry fit between the congruent pair and therefore described by the 24 shifts all of which were measured independently. Thus the \mathbf{P} matrix has a dimension of 24×12 . The derivatives were estimated by finite differences by changing each spectral point by the average line width, ± 0.7 ppm, in the fitting routine.

The results of this analysis in the molecular frame indicate an average uncertainty, expressed as one marginal deviation, of 0.38 ppm for the principal values and $\sim 0.3^\circ$ in the angles. The uncertainty in the various principal values range from 0.30 to 0.45 ppm in reasonable agreement with the overall composite error. The uncertainty in the directional cosines depends critically upon the corresponding difference among the principal components. As a result of the small anisotropy between the two in-plane bridgehead components, the orientations of δ_{11} and δ_{22} of the four bridgehead tensors, C_{3a} , C_{9a} , C_{9b} , and C_{12c} , have very large uncertainties and these axes are essentially undefined in the aromatic plane. On the other hand, δ_{33} and their directions for all tensors are well-defined as a result of the large anisotropy between δ_{33} and both δ_{11} and δ_{22} . The corresponding uncertainty in the δ_{33} directional cosine for $\cos \theta_N$ is of the order of 0.1° while the average uncertainties for $\cos \theta_L$ and $\cos \theta_M$ of δ_{33} are less than 0.3° for all the observed tensors. This value is an order of magnitude smaller than the differences among the directional cosines of δ_{33} reported in Table 2 for chemically similar tensors. As discussed above, this high precision in the

(27) As pointed out by a referee the lack of definite assignments in some cases is an unavoidable shortcoming of this paper. We acknowledge this problem, but unfortunately none of the traditional assignment tools commonly used for liquid spectra—INADEQUATE, selective labeling, etc.—are fully applicable in the solid state, because the lack of resolution and sensitivity or unfavorable relaxation times precludes their use here.

Table 3. Distances¹⁴ between Calculated and Experimental Chemical Shift Tensors^a

geometry	rms
X-ray	6.4
X-ray with D_{2h} symmetry ^b	5.4
X-ray with C_{2v} symmetry ^b	5.0
X-ray with C_2 symmetry ^b	5.1
X-ray with optimized protons	5.4
full optimization (D_{2h})	4.5
C_{2v} (D_{2h} with bent carbons)	4.0
C_{2v} (D_{2h} with bent β hydrogens)	4.0

^a Values in ppm calculated as described in ref 14. X-ray geometry from ref 19. ^b The hydrogen positions were optimized after averaging the X-ray carbon positions with the imposed symmetry.

measurements enables the resonances of the chemically similar nuclei to be resolved. This precision allows the use of the observed tilting of the δ_{33} orientations as a means for assigning, at least tentatively, otherwise very similar tensors.

Discussion

Crystalline Effects on Chemical Shift Tensors. The distortion of perylene from the idealized D_{2h} symmetry is revealed by principal shift values that differ as much as 5 ppm and by isotropic shift values, δ_{iso} , that differ up to 3.6 ppm for similar carbons. The residuals between the measured tensors and their averaged values to different symmetry constraints are 1.05, 1.47, and 2.30 ppm for C_2 , C_{2v} and D_{2h} , respectively. While these distances are modest they are significant as they are three or more marginal standard deviations greater than the composite error, 0.30 ppm, in the measurement. Possible explanations of these measurable effects between the chemically similar tensors include differential vibrational motions, minor structural deformations, and direct intermolecular shift effects. The last effect has previously been estimated to be about 1 ppm, which could be a significant contribution to the observed reductions in the NMR symmetries,^{7,8} but not enough to fully explain the effects observed here.

(a) Structural Variation. The X-ray structure of perylene exhibits relatively large deviations from the D_{2h} molecular symmetry, but they are generally within or close to the uncertainty of the diffraction measurements. Calculated tensors using X-ray geometries obtained by averaging the structural parameters to satisfy the D_{2h} , C_{2v} , and C_2 molecular symmetry followed by the optimization of the proton positions, to correct for the well-known deficiency in the X-ray method to locate their positions, results in rms distances reported in Table 3. Imposing the above symmetries on the X-ray geometries does not significantly improve the overall rms distances. A closer examination of the individual shift distance reveals a large discrepancy for the outer bridgehead positions, C_{3a} and C_{9a} of 8.58 and 6.94 ppm, respectively, for all of these imposed symmetries. This is consistent with the observation that the second largest variation, 0.024 Å, in C–C bond length that affects the shifts is between the outer α and outer bridgehead positions. The significant improvement observed when the proton positions are optimized is a clear confirmation of this well known deficiency of the X-ray technique. The comparable rms for different symmetrized structures indicates that the lack of precise knowledge of the molecular structure is an important source of limitation in the calculations, but current limitation in the modeling precludes at this time the use of the NMR data to obtain the molecular structure.

The X-ray structure of perylene in the α form suggests a significant and systematic bending from a planar structure. The corresponding tensors also reveal δ_{33} orientations that deviate

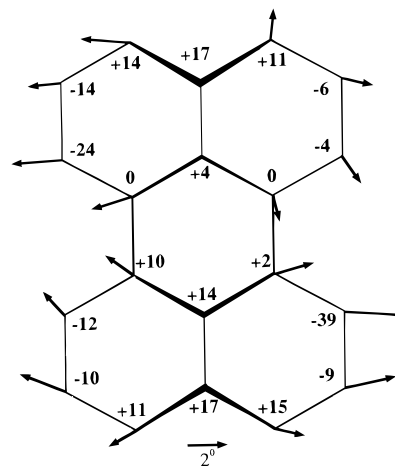


Figure 5. Tilting of δ_{33} principal components. The vectors in the figure represent the direction, $\tan^{-1}(\delta_{33} \cos \theta_L / \delta_{33} \cos \theta_M)$, of the individual δ_{33} tilt from the average δ_{33} and the magnitude of the vectors, $\cos^{-1}(\delta_{33} \cos \theta_M)$, corresponds to the angle between the individual δ_{33} and the average δ_{33} . The positions of the carbon nuclei reported in the X-ray study with respect to the best fit carbon plane are also shown here in units of 10^{-3} Å.

from the average δ_{33} directions in a way that is compatible with the X-ray data. Figure 5 shows the projection of the δ_{33} tilt onto the molecular plane. This feature was used to make the tensor assignments as discussed above and provides an empirical link between the X-ray and NMR results. Starting with a fully optimized D_{2h} structure, the carbon positions were first bent in 1° increments about the L axis of the molecule so as to form various angles between the A/B and C/D sections of the molecule. An angle of $2-3^\circ$ produces the least rms distance, 4.0 ppm, in the calculated vs experimental correlation. Alternatively, systematically bending the hydrogens can also model the tilting of δ_{33} in the experimental tensors until an rms distance of 4.0 ppm is also achieved. In the case of bending individual hydrogens out of plane, the tilt of δ_{33} projects along the corresponding C–H bond, and to rationalize the observed directional cosines for δ_{33} , all four β hydrogens must bend in the same manner while leaving the outer α hydrogens in the plane. Therefore, the most plausible explanation for the systematic tilt observation δ_{33} is a combination of both carbon and hydrogen deformations from the average aromatic plane.

(b) Vibrational Motion. The influence of vibrational motion on the chemical shift may be estimated by a Taylor expansion about the equilibrium geometry,²⁸

$$\langle \delta \rangle \cong \delta_e + \sum_i \left. \frac{\partial \delta}{\partial \rho_i} \right|_e (\rho_i - \rho_e) + \frac{1}{2} \sum_{ij} \left. \frac{\partial^2 \delta}{\partial \rho_i \partial \rho_j} \right|_e \langle (\rho_i - \rho_e)(\rho_j - \rho_e) \rangle + \dots \quad (4)$$

where $\langle \delta \rangle$ is the expectation value of the chemical shift, δ_e is the shift at the equilibrium structure, and $(\partial \delta / \partial \rho_i)_e$ and $(\partial^2 \delta / \partial \rho_i \partial \rho_j)_e$ are the first and second derivatives of shift with respect to the internal displacement coordinates, ρ_i , evaluated at the equilibrium position. The contributions from each higher order term is estimated to decrease by approximately an order of magnitude²⁹ and therefore only the first non-zero terms need be considered. For the vibrational modes for which $\partial \delta / \partial \rho \neq 0$, the first-order contributions arise from the anharmonic contributions to ρ_i , because the harmonic contributions to $\langle \rho_i \rangle_{\text{Har}}$ are 0. When the shielding is a symmetric function of the

(28) Jameson, C. J. *Bull. Magn. Reson.* **1980**, 3, 3.

(29) Jameson, C. J. *J. Chem. Phys.* **1977**, 66, 4977.

coordinate ρ_i , as in the out of plane vibration, $\partial\delta/\partial\rho_i = 0$, and therefore the first non-zero contribution arises from the second-order harmonic contributions to $\langle\rho_i\rho_j\rangle_{\text{Har}}$ which are not necessarily zero.

To simplify the calculation of the vibrational estimates, the derivatives of chemical shift with respect to internal coordinates were taken from the previously calculated values for naphthalene, where they were estimated by finite differences.⁸ The derivatives are found to be quite large for C–C and C–H bond changes, up to ~ 250 and ~ 125 ppm/Å, respectively, and ~ 2.5 and ~ 1.0 ppm/deg for C–C–C and C–C–H angular deformation, respectively. The out-of-plane C–H vibrations give theoretical derivatives of ~ 1.5 ppm/deg. Similar numerical derivatives were also obtained for acenaphthene¹ and therefore it is assumed that a particular carbon geometry dominates these shielding derivatives. It appears that such derivatives are transferable from molecule to molecule when the local structure is comparable.

The absence of anharmonic vibrational information on perylene required the use of corresponding anharmonic vibrational averages for benzene at 300 K.³⁰ The overall effect on the shifts from stretching motions is estimated to be as large as 3.0 ppm for in-plane diagonal components, δ_{LL} and δ_{MM} , and 2.0 ppm for the out-of-plane diagonal component δ_{NN} . For the off-diagonal components, δ_{LM} , δ_{MN} , and δ_{NL} , the estimate exhibits corrections as large as 0.5 ppm. These estimates are of the same order of magnitude as reported for the rovibrational corrections to the ¹³C shielding in methane at 300 K, i.e., -3.3 ppm.³¹ For angular deformations, no anharmonic vibrations were reported for benzene. In order to have an equivalent effect on the shift as the bond stretches, the C–C–C and C–C–H angular anharmonic vibrational deformations would need to be of the order of $\sim 0.5^\circ$, a value that approximates their total in-plane angular motions. Therefore, stretching deformations are expected to exceed anharmonic angular vibrations in their effect on chemical shift tensors measured at room temperature. Further, the shift derivative at the equilibrium position for angular harmonic motions is zero and for such vibrations only higher even order harmonic corrections contribute to the averaging. These contributions may be significant especially in the out-of-plane hydrogen harmonic vibrations, which on average are as large as 7° for naphthalene.³² Such out-of-plane vibrations are estimated to affect the shift by 5 ppm or more. All of these vibrational corrections include zero order as well as higher order terms, and would have to be considered in a complete vibrational correction analysis.

Based on these simple considerations, vibrational effects on shifts cannot be ignored, and indicate that all three mechanisms—direct intermolecular effects, small local geometrical deformations, and differential thermal averaging—could be of similar magnitude. By contributing in a cooperative fashion, the variation observed in the chemical shifts of chemically similar but crystallographically different chemical shift tensors may be explained.

The Electronic Structure of Perylene. The in-plane components of the chemical shift tensor, δ_{11} and δ_{22} , for aromatic molecules are very sensitive to the π -electronic structure and the anisotropy between δ_{11} and δ_{22} reflects the nonsymmetrical distribution of π -electrons in the vicinity of the nucleus. It has been demonstrated³³ that the in-plane anisotropy

parallels the difference in bond orders of the three bonds directly attached to condensed sp^2 carbons. Both inner and outer bridgehead positions (C_{3a}, C_{3b}, C_{9a}, and C_{12c}) exhibit very small in-plane anisotropy indicating a symmetrical π -electron distribution. The 0.4 ppm $\delta_{11} - \delta_{22}$ anisotropy observed for the C_{9a} is smaller than any other observed in PAH molecules studied previously.

According to bond order calculations, the three bonds directly attached to the inner α carbons have various amounts of π -character and the maximum difference is 0.40 electron.³³ Consequently, the corresponding in-plane anisotropy for these inner α positions is ~ 60 ppm, indicating that a significant anisotropy exists in the π -electron distribution and that the π -electrons remain essentially localized in the naphthalene fragments. Moreover, the δ_{22} shift of these carbons is nearly identical to those of tetramethylnaphthalene,¹⁸ suggesting that the peri-bonds behave as biaryl linkages and not as typical bridgeheads. This conclusion is consistent with the simple Kekule description of perylene and is also supported by the long, 1.471 Å, peri-bond length.

To analyze the dependence of π -character on local molecular geometry, chemical shielding calculations were executed with an idealized aromatic perylene structure, i.e. all C–C and C–H distances and bond angles were set to 1.39 Å, 1.08 Å, and 120° , respectively. The resulting in-plane anisotropy at the inner α positions still remained large, 74 ppm, while that of the bridgehead tensors remained small, 6–13 ppm. Hence, it is apparent that the distribution of π -electrons is largely determined by the molecular connectivities and not by the particular bond lengths. One therefore must be careful in making conclusions about the aromaticity of a particular bond based solely on its corresponding bond length. The long peri-bond in perylene can be attributed at least in part to the reduction of the intramolecular strain between the inner β hydrogens. Because of the small π -character in the C_{6a}–C_{6b} and C_{12a}–C_{12b} bonds, it is energetically more favorable to elongate them than to distort significantly the planarity of the molecule as it is observed in phenanthrene.³⁴

The 17-ppm difference in the shift of δ_{11} between the inner and outer β positions reflects a neighboring center ring. The δ_{11} shift to lower frequencies for a β carbon near an additional ring is observed in acenaphthene, 211 ppm,¹ and pyracene, 209 ppm,¹⁸ both similar to that in perylene, 213 ppm. The outer β δ_{11} shift of perylene, 230 ppm, closely resembles the shift of the β positions furthest from the neighboring ring in acenaphthene,¹ 231 ppm, and in the β positions in both naphthalene,¹⁶ 228 ppm, and tetramethylnaphthalene,¹⁸ 235 ppm. Comparisons between the structures of acenaphthene, and perylene suggest that these β shifts are not correlated well with bond lengths, angles, or bond orders. Interestingly, the quantum mechanical calculations follow the experimental trend as a difference of 20 ppm is calculated between δ_{11} for the two types of β positions in perylene.

In perylene the averaged δ_{33} for the outer β positions and inner β positions is 10.6 and 8.5 ppm, respectively, and this modest 2 ppm lower frequency shift on δ_{33} of the inner β positions can be attributed to the steric interactions between the intramolecular bay hydrogens, as is observed for the α positions in phenanthrene.¹⁷ A value of 11–14 ppm has been observed for δ_{33} shift components of carbons β to a bridgehead carbon in naphthalene,¹⁶ 1,2,3,6,7,8-hexahydroxyrene,¹⁸ 1,4,5,8-tetramethylnaphthalene,¹⁸ and acenaphthene.¹ In pyracene¹⁸ the δ_{33} shift is 19 ppm and only in pyrene,¹⁵ where carbons are

(30) Lounila, J.; Wasser, R.; Diehl, P. *Mol. Phys.* **1987**, 62 19.

(31) Jameson, C. J.; Osten, H. J. In *Annual Reports on NMR Spectroscopy*; Webb, G. A., Ed.; Academic Press: London, 1986; Vol. 17, p 2.

(32) Cyvin, S. J.; Cyvin, B. N.; Hagen, G.; Cruickshank, D. W. J.; Pawley, G. S. In *Molecular Structures and Vibrations*; Cyvin, S. J., Ed.; Elsevier: New York, 1972; p 299.

(33) Facelli, J. C.; Grant, D. M. *Theor. Chim. Acta* **1987**, 71, 277.

(34) Ferraris, G.; Jones, D. W.; Yerkess, J. Z. *Krist.* **1973**, 138, 113.

simultaneously β to two bridgehead carbons, is the δ_{33} less than 11 ppm. Therefore the steric interactions seem to be the most likely explanation for the small shifts observed in the δ_{33} components of the inner β carbons.

Conclusions

Single-crystal NMR data contain a wealth of information on the molecular structure of solids. As demonstrated with the 40 chemical shift tensors of perylene determined within 0.30 ppm, the method of ^{13}C CS-CS correlation spectroscopy allows the tensor determination of crystal structures with numerous magnetically different nuclei. The crystal symmetries even for larger crystals such as perylene provide shift values with no loss in accuracy.

For aromatic systems, chemical shift tensors provide a measure of the delocalization of π electrons. In perylene, the tensors at the peri-positions, C_{6a} , C_{6b} , C_{12a} , and C_{12b} , reveal lower δ_{22} shifts similar to the shifts for the substituted positions in 1,4,5,8-tetramethylnaphthalene. This indicates that the π -electron delocalization remains primarily within each naphthalene residue.

Solid state distortions in perylene are readily observed in the spectra with splittings of up to 11 ppm between shifts assigned

to carbon positions related through the molecular center. The overall 1.47-ppm rms distance between the tensors of chemically similar positions assuming the molecule exhibits C_{2v} symmetry is also a clear indication of these effects, because this distance is well above the estimated uncertainty of the measurements. The most noted crystalline distortion is the systematic tilt in the orientation of δ_{33} at the β positions, which supports the diffraction observation of perylene bending about the long axis of the molecule. The smallest effects on the shifts cannot be traced to specific deformations in the molecular structure and may have significant contributions from direct intermolecular effects and differential thermal averaging.

Acknowledgment. This work was supported by the Basic Energy Sciences Program at the Department of Energy under Grant No. DE FG02-94ER14452 and by computer resources from the University of Utah Supercomputing Institute. The authors are grateful for a copy of the TX93 program obtained from Professors Wolinski, Hinton, and Pulay and to Dr. D. W. Alderman for the software to process the chemical shift tensor data.

JA954052D